Vol 18 No 1, January 2009
1674-1056/2009/18(01)/0287-06

Chinese Physics B

© 2009 Chin. Phys. Soc.
and IOP Publishing Ltd

Quick preparation and thermal transport properties of nanostructured β-$FeSi_2$ bulk material*

Li Han(李 涵), Tang Xin-Feng(唐新峰)†,
Cao Wei-Qiang(曹卫强), and Zhang Qing-Jie(张清杰)

State Key Laboratory of Advanced Technology for Materials Synthesis and Processing, Wuhan University of Technology, Wuhan 430070, China

(Received 8 April 2008; revised manuscript received 20 May 2008)

This paper reports that the nanostructured β-$FeSi_2$ bulk materials are prepared by a new synthesis process by combining melt spinning (MS) and subsequent spark plasma sintering (SPS). It investigates the influence of linear speed of the rolling copper wheel, injection pressure and SPS regime on microstructure and phase composition of the rapidly solidified ribbons after MS and bulk production respectively, and discusses the effects of the microstructure on thermal transport properties. There are two crystalline phases (α-Fe_2Si_5 and ε-FeSi) in the rapidly solidified ribbons; the crystal grains become smaller when the cooling rate increases (the 20 nm minimum crystal of ε-FeSi is obtained). Having been sintered for 1 min above 1123 K and annealed for 5 min at 923 K, the single-phase nanostructured β-$FeSi_2$ bulk materials with 200–500 nm grain size and 98% relative density are obtained. The microstructure of β-$FeSi_2$ has great effect on thermal transport properties. With decreasing sintering temperature, the grain size decreases, the thermal conductivity of β-$FeSi_2$ is reduced remarkably. The thermal conductivity of β-$FeSi_2$ decreases notably (reduced 72% at room temperature) in comparison with the β-$FeSi_2$ prepared by traditional casting method.

Keywords: thermoelectric materials, nanostructure, thermal conductivity
PACC: 7215, 6140M, 7430F

1. Introduction

Semiconducting iron disilicide, β-$FeSi_2$, is one of the potential candidates for practical use in the high temperature range (up to 1200 K) thermoelectric materials because of its high Seebeck coefficient, its abundance as a raw material and good resistance to oxidation.[1−14] However, the thermal conductivity of β-$FeSi_2$ is still high, so the figure of merit of its thermoelectric properties is low for practical use in comparison with other thermoelectric materials. Moreover, it costs a long time to prepare β-$FeSi_2$ bulk material by using traditional technology, for example, for the pure as-cast $FeSi_2$, more than 100 h anneal time is needed to form the complete β-$FeSi_2$ phase at 1073 K.[1] The long annealing process increases the preparation periods and costs, and grain grows markedly during the process, which is not good for the decrease of the thermal conductivity of β-$FeSi_2$ and for the optimization of the thermal performance. Therefore, the research and exploration of a new, quick preparation process by which we can obtain nanostructured β-$FeSi_2$material are of great importance to the improvement of thermoelectric properties.

Figure 1 is the binary phase diagram of the Fe–Si system (Kubaschewski 1982),[2] which shows that the stoichiometric $FeSi_2$ alloy solidifies at 1485 K as a eutectic structure composed of α-Fe_2Si_5 and ε-FeSi phases. The β-$FeSi_2$ phase is formed by the peritectoid reaction of the two eutectic phases below 1255K. Because of the limited solid solubility of β-$FeSi_2$ phase and stacking fault that occurs during the peritectoid reaction, the rate of β- $FeSi_2$ phase transformation is very slow.[7,8] It is expected that grain refinement of the α and ε phases can accelerate the formation of the β phase and improve the thermoelectric performance of β-$FeSi_2$.[2,10] It has been shown that rapid solidification is very effective for the production of a fine crystalline microstructure.[2,10−12,15−16] In recent researches, Chen *et al*[11,12] have prepared n-type $Fe_{0.94}Co_{0.06}Si_{2.00}$ and p-type $Fe_{0.92}Mn_{0.08}Si_x$ by rapid solidification (the melt was sputtered onto the edge of

*Project supported by the 973 Project (Grant No 2007CB607501), the National Science Foundation of China (Grant No 50572082) and the Cultivation Fund of the Key Scientific and Technical Innovation Project of China (Grant No 705035).
†E-mail: tangxf@whut.edu.cn

a chilled rolling molybdenum wheel) and hot pressing; the performance of β-$FeSi_2$ based materials has been improved notably and the preparation period is effectively reduced.

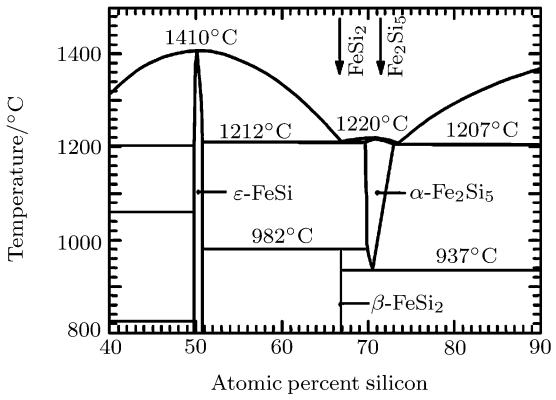


Fig.1. Binary phase diagram of the Fe-Si system (Kubaschewski 1982).

In order to eliminate the influence on thermoelectric properties and structure induced by foreign atoms, pure iron disilicide is chosen as a start material, and melt spinning (MS) is applied to produce the nanostructured and α, ε phases evenly dispersed thin ribbons. Effects of MS process on morphologies and distribution of α, ε phases are studied. The milled ribbons are sintered into single β-$FeSi_2$ phase by spark plasma sintering (SPS) technique which makes sintering and annealing process complete within relatively short time and low temperature and avoids excessive growth of grains. The influence of SPS regime on β phase transformation and microstructure of bulk materials are investigated, and the relationship between microstructure of β-$FeSi_2$ and thermal transport properties is revealed.

2. Experiments

Highly pure metals of Fe (99.99%, ingot) and Si (99.9999%, bulk) were used as starting materials. The constituent elements were weighed according to the $FeSi_2$ formula and melted in an arc furnace for 3–4 times, and then the ingots were put into a quartz cylinder in MS system to induce melt. The melt was rapidly solidified after being injected onto the edge of a chilled rolling copper wheel at a linear speed of about 10–30 $m \cdot s^{-1}$. Both arc melting and rapid solidification were carried out under a high purity argon atmosphere (>99.99%). The rapidly solidified thin ribbons were milled in a carnelian mortar into fine powder, and then the powder was loaded into a graphite die and sintered by SPS method. Sintering temperature and time are 923–1173 K and 5 min respectively, and single-phase, nanostructured β-$FeSi_2$ bulk materials were then obtained.

The constituent phases of the samples were determined by powder x-ray diffractometry (PANalytical: X' Pert PRO, Cu Kα). Densities of the samples were measured by using the Archimedes method. The fine microstructure of the ribbon after MS and morphologies of bulk material sintered by SPS were observed by field emitted scanning electron microscopy (FESEM) (Sirion 200 FESEM). The thermal conductivity (κ) was calculated from the measured thermal diffusivity D, specific heat C_p, and density d by using the relationship $\kappa = DC_pd$. D and C_p were measured by the laser flash method (Sinkuriko: TC-7000) in a vacuum. All the measurements were performed under the temperature range from 300 to 800 K.

3. Results and discussion

3.1. Synthesis and structure of thin ribbons prepared by MS

Figure 2 shows the x-ray diffraction (XRD) patterns of the ribbons prepared by different MS regimes. As seen in Fig.2, all the ribbons are composed of α-Fe_2Si_5 and ε-FeSi phases and no β-$FeSi_2$ phase occurs.

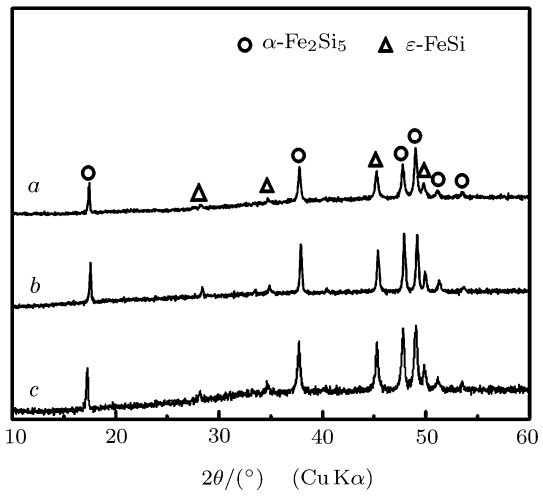


Fig.2. X-ray diffraction patterns of the ribbons prepared by different MS regime: curve *a* linear speed: 10 m/s, injection pressure: 0.02 MPa; curve *b* linear speed: 30 m/s, injection pressure: 0.1 MPa; curve *c* linear speed: 30 m/s, injection pressure: 0.02 MPa.

The widening of diffraction peaks and low diffraction intensity are caused by the fine grains size of α and ε phases (nano-scale, see Fig.3).

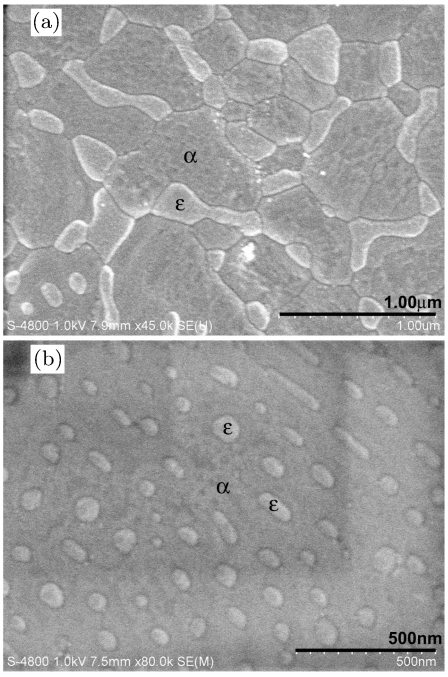


Fig.3. Free face FESEM photographs of the ribbons prepared by different linear speed of copper wheel with the same injection pressure of 0.02 MPa: (a) 10 m/s; (b) 30 m/s.

For convenience, we define the side which contacts with the edge of the copper wheel of the ribbons as contact face, and the other side as free face. As for MS rapid solidification, cooling rate is adjusted and controlled mainly by the regulation of the linear speed of the rolling copper wheel and injection pressure of the quartz cylinder nozzle. Figure 3 shows the free face FESEM photographs of the ribbons prepared by changing the linear speed of copper wheel from 10 to 40 m/s under the same injection pressure of 0.02 MPa. A eutectic structure consisting of dark matrix being α-Fe_2Si_5 and white ε-FeSi phases which are confirmed by energy dispersive x-ray (EDX) analysis and XRD (see Fig.2) can be seen in Figs.3(a) and 3(b). Figure 3(a) shows the morphology of free face of the ribbon when the linear speed of copper wheel is 10 m/s. As shown in the figure, the white granular ε phase possesses a grain dimension changing from 200 nm to 1 μm, while the dark dendritic α phase shows a random orientation. These results are very similar to those of Ref.[10]. When the linear speed increases to 30 m/s, as shown in Fig.3(b), the granular ε phase exhibits more fine grain size with 20–70 nm , and evenly disperses in the α matrix; the dendritic α phase does not occur. The cooling rate increases with the increase of linear speed of rolling wheel, when linear speed reaches 30 m/s. The melt is cooled by an extraordinarily high cooling rate. Liquid–solid boundaries are impelled speedily and atomic long-range diffusion is restrained, as a result, the crystallization process terminates before the further growth of grains, and then the nano-scale eutectic structure of ε and α phases forms.

Figure 4 shows the free face FESEM photographs of the ribbons prepared by changing the injection pressure from 0.02 to 0.1 MPa with the same linear speed of the copper wheel of 30 m/s. As shown in Fig.4, with the increase of the injection pressure, the grains of ε phase grow remarkably, when the injection pressure increases to 0.1 MPa. It can be seen in Fig.4(c) that rough dendritic ε and α phases have formed. This

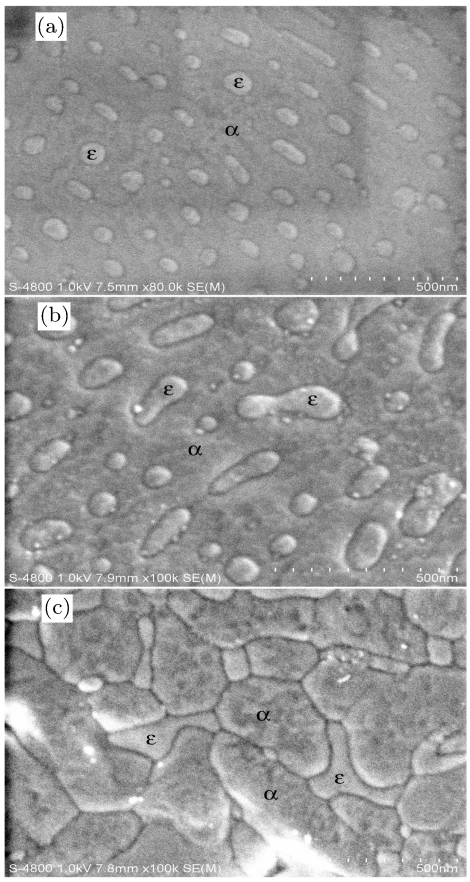


Fig.4. Free face FESEM photographs of the ribbons prepared by different injection pressure with the same linear speed of copper wheel of 30 m/s: (a) 0.02 MPa; (b) 0.06 MPa; (c) 0.10 MPa.

is mainly due to the fact that increase of the ejection pressure results in increase of the contact time (length) between the ribbon and the wheel surface which provides further evidence of improved heat transfer conditions. According to the morphology analysis of the free face of thin ribbons, fine grains of ε phase which is evenly dispersed in the α matrix can be obtained when linear speed of copper wheel and injection pressure are 30 m/s, 0.02 MPa respectively.

As shown in Fig.1, for the sample that is weighed according to stoichiometric $FeSi_2$, β phase forms at the boundaries of ε and α phases by the peritectoid reaction. With the growth of β phase, atomic diffusion length increases and the time for completing peritectoid reaction lengthens, as a result the fine grains of ε and α eutectic phases which effectively augment the amount of boundaries can accelerate the formation of the β phase.[8,9] In comparison with traditional fusion casting[1] and rapid solidification (in which the melt is cooled by a chilled rolling molybdenum wheel) method,[12] ε and α phases show more fine grains size (20–70 nm, see Fig.3(b)). As it is mentioned above, nanostructured β phase is expected to form at relatively short time and low temperature.

3.2. Quick preparation and microstructure of bulk β-$FeSi_2$

Figure 5 shows the XRD patterns of the bulk materials sintered by different SPS regime using the milled ribbons prepared under the same MS regime (linear speed: 30 m/s; injection pressure: 0.02 MPa). Curve *a* in Fig.5 shows when the ribbons are sintered at 1023 K for 5 min, the single-phase β-$FeSi_2$ has formed, but the relative density of the sample is just 85%. When the ribbons are sintered at 1073 K for 5 min, as seen in the figure, ε and α phases have formed; therefore, the increase of sintering temperature may lead to the decomposition of β-$FeSi_2$. When the ribbons are sintered at 1123 K and 1173 K for 1min respectively and annealed at 923 K for 5 min, as we can see curves *c* and *d* in Fig.5, the single-phase β-$FeSi_2$ is obtained and the relative density of the sample is above 98%. In comparison with traditional fusion casting and rapid solidification combined with hot pressing method,[1,11,12] single-phase β-$FeSi_2$ bulk materials sintered by SPS are obtained at the low temperature and within the short time, this process is beneficial to restrain the growth of β-$FeSi_2$ phase grain.

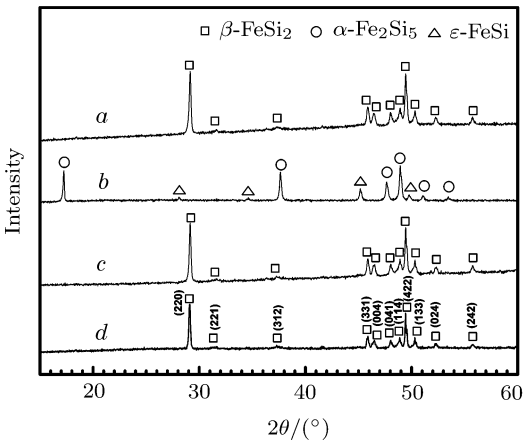


Fig.5. X-ray diffraction patterns of the bulk $FeSi_2$ materials sintered by different SPS regime: curve *a* 1023 K× 5 min; curve *b* 1123 K× 5 min; curve *c* 1123 K×1 min + 923 K×5 min; curve *d* 1173 K ×1 min+ 923 K×5 min.

The FESEM micrographs of bulk β-$FeSi_2$ sintered by different SPS regime using the milled ribbons prepared under the same MS regime (linear speed: 30 m/s; injection pressure: 0.02 MPa) are shown in Fig.6. When the sample was sintered at 1123 K for 1 min and annealed at 923 K for 5 min, the dimension of fine grains is 200–500 nm; the sample sintered

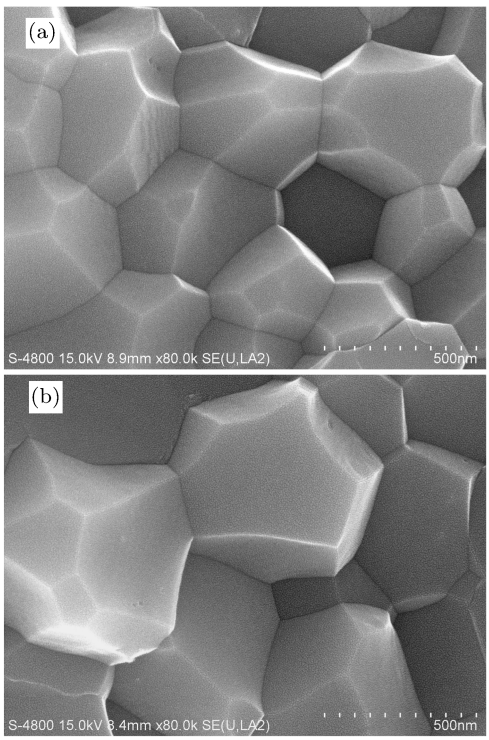


Fig.6. FESEM micrographs of bulk β-$FeSi_2$ sintered by different SPS regime: (a) 1123 K×1 min+923 K×5 min; (b) 1173 K×1 min+923 K×5 min.

at 1173 K for 1 min and annealed at 923 K for 5 min shows an obvious growth of grains with dimension of 400–600 nm at the higher sintering temperature. Furthermore, since ribbons are milled into powders for the subsequent SPS process, the different microstructure of the ribbon samples would have important impact on the characteristic microstructure of the bulk β-$FeSi_2$ materials.

Figures 7(a) and (b) show the FESEM micrographs of bulk β-$FeSi_2$ sintered by the same SPS regime (1123 K×1 min+923 K×5 min) using the milled ribbons prepared under the different MS regime ((a): linear speed: 30 m/s, injection pressure: 0.02 MPa; (b): linear speed: 30 m/s, injection pressure: 0.1 MPa). The granular grains with homogeneous dimension can be seen in Fig.7(a), but rough prismatic grains are formed in Fig.7(b). According to Fig.4, while the injection pressure is 0.02 MPa, granular grains of ε phase are evenly dispersed in α phase matrix (see Fig.4(a)), and when the injection pressure increases to 0.1 MPa, ε and α phases have grown into rough dendritic crystals (see Fig.4(c)), as a result, the grains of β-$FeSi_2$ show granular and columnar shape respectively.

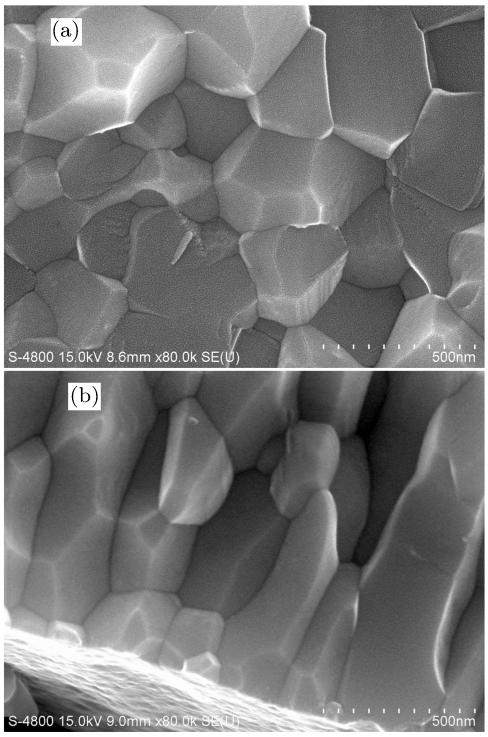


Fig.7. FESEM micrographs of bulk β-$FeSi_2$ sintered by same SPS regime using the ribbons prepared by different MS regime: (a) 30 m/s, 0.02 MPa; (b) 30 m/s, 0.10 MPa.

A conclusion can be drawn that ε and α phases can be completely transformed into β phase by SPS process within short time, and fine grains of β-$FeSi_2$ can be obtained when the ε and α phases possess fine grains and these phases are evenly dispersed in the ribbon samples. Moreover, these nanostructures induce a large number of interfaces which may have great effects on the thermal transport properties of materials.

3.3. Thermal transport properties of bulk β-$FeSi_2$

Influences of different microstructures on thermal conductivity are studied, and the results are compared with those obtained by traditional casting and rapid solidification combined with hot pressing method. All the samples in this section are prepared by the same MS parameters (linear speed: 30 m/s, injection pressure: 0.02 MPa) but different SPS sintering parameters. As seen in Fig.8, the thermal conductivity of sample d changes from 4 to 3.2 $W \cdot m^{-1} \cdot K^{-1}$ which is less than the thermal conductivity of sample c (5.8–4.2 $W \cdot m^{-1} \cdot K^{-1}$) at the tested temperature range, that is to say the thermal conductivity increases with the increase of sintering temperature. This can be explained by the fact that the grains grow bigger when the sintering temperature increases, (seen in Fig.6) so the number of boundaries decreases for unit volume and the scattering effect on phonons weakens. In comparison with the thermal conductivity obtained by fusion casting method,[1] thermal conductivity in this research (sample d) decreases from 14.2 to 4 $W \cdot m^{-1} \cdot K^{-1}$ (reduced 72%) at room temperature, and the thermal

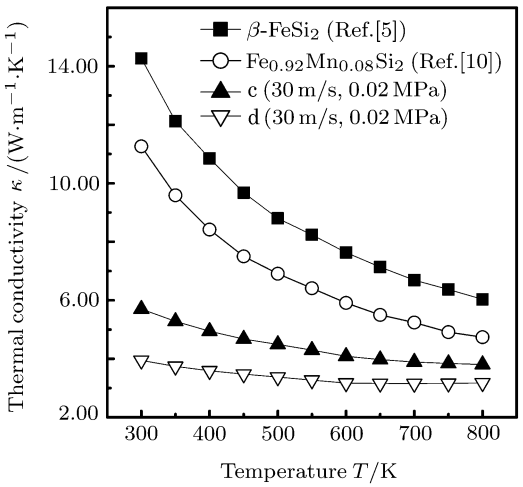


Fig.8. Thermal conductivities of bulk β-$FeSi_2$ materials prepared by different methods: ■ fusion casting method; ○ rapid solidification combined with hot uniaxial pressing method; ▲ SPS: 1173 K×1 min+923 K×5min; ▽ SPS: 1123 K×1 min+923 K×5 min.

conductivity decreases from 6.3 to 3.2 $W \cdot m^{-1} \cdot K^{-1}$ (reduced 50%) at 800 K. The thermal conductivity in this research decreases notably in comparison with the thermal conductivity[12] of Mn doped β-$FeSi_2$ obtained by rapid solidification combined with hot pressing method too. As for doped β-$FeSi_2$ material, the substitution of Fe site by Co or Mn results in a drastic disorder of the crystal lattice and lattice thermal conductivity can be further reduced.[5−20] The higher thermoelectric performance is expected to be achieved in doped β-$FeSi_2$ material prepared by using MS+SPS method.

4. Conclusions

In conclusion, nanostructured single-phase β-$FeSi_2$ bulk materials are prepared by combining MS and SPS method. The influences of MS and SPS parameters on the phase transformation, the microstructure of ribbons and bulk materials are investigated. The relationship between microstructure of β-$FeSi_2$ and thermal transport properties is revealed so that the following conclusions can be drawn.

(1) All the ribbons after MS are composed of α-Fe_2Si_5 and ε-FeSi phases; grain dimension of α and ε phase decreases with the increase of the linear speed of the rolling wheel or the decrease of injection pressure, ε phase is more homogeneous dispersed in the α phase matrix. When the linear speed and injection pressure are 30 m/s and 0.02 MPa respectively, the granular ε-FeSi phase possesses a nano-scale of 20–70 nm and is homogeneously dispersed in α-Fe_2Si_5 matrix. This special structure is beneficial to the quick transformation of β-$FeSi_2$ at subsequent SPS process.

(2) After being sintered for 1 min above 1123 K and annealed for 5 min at 923 K, the single-phase nanostructured β-$FeSi_2$ bulk materials with 200–500 nm grain size and 98% relative density are obtained. In comparison with traditional fusion casting and rapid solidification combined with hot pressing method,[1,11,12] single-phase β-$FeSi_2$ bulk materials sintered by SPS are obtained at the low temperature and within the short time. The different microstructures of the ribbon samples would have important impact on the characteristic microstructure of the bulk β-$FeSi_2$ materials, and fine grains of β-$FeSi_2$ can be obtained when the ε and α phase possess fine grains and evenly dispersed in ribbon samples.

(3) The thermal conductivity of samples in this research changes from 3 to 6 $W \cdot m^{-1} \cdot K^{-1}$ which is remarkably less than the thermal conductivity obtained by fusion casting method[1] at the testing temperature range. The thermal conductivity is reduced 72% at room temperature and 50% at 800 K. The higher thermoelectric performance is expected to be achieved in doped β-$FeSi_2$ material prepared by MS+SPS method.

References

[1] Nishida I 1973 *Phys. Rev.* B **7** 2710
[2] Kubaschewski O 1982 *Iron Binary Phase Diagram* (New York: Springer) p136
[3] Nagai H 1995 *Mater. Trans. JIM* **136** 363
[4] Li X N, Nie D, Dong C, Ma T C, Jin X and Zhang Z 2002 *Acta Phys. Sin.* **51** 115 (in Chinese)
[5] Wang H Y, Liu R P, Ma M Z, Gao M, Yao Y S and Wang W K 2004 *Acta Phys. Sin.* **53** 2378 (in Chinese)
[6] Kojima T 1989 *Phys. Status Solidi* A **111** 233
[7] Kojima T, Shkata M and Nishida I 1990 *J. Less-Common Metals* **159** 299
[8] Zhao X B, Zhu T J, Hu S H, Zhou B C and Wu Z T 2000 *J. Alloys Compd.* **306** 303
[9] Negase T, Yamauchi I and Ohnaka I 2000 *J. Alloys. Compd.* **312** 295
[10] Nagai T, Yamauchi I and Ohnaka I 2000 *J. Alloys Compd.* **312** 295
[11] Chen H Y, Zhao X B, Lu Y F, Mueller E and Mrotzek A 2003 *J. Appl. Phys.* **94** 6621
[12] Chen H Y, Zhao X B and Stiewe C 2007 *J. Alloys Compd.* **433** 338
[13] Yamauchi I, Okamoto T, Ohata H and Ohnaka I 1997 *J. Alloys Compd.* **260** 162
[14] Ito M, Tanaka T and Hara S 2004 *J. Appl. Phys.* **95** 6209
[15] Zhu T J, Zhao X B and Hu S H 2001 *J. Mater. Sci. Lett.* **20** 1831
[16] Tani J I and Kido H 2000 *Jpn. J. Appl. Phys.* Part 1 **39** 1054
[17] Pan Z J, Zhang L T and Wu J S 2005 *Acta Phys. Sin.* **54** 5308 (in Chinese)
[18] Umemoto M 1995 *Mater. Trans. JIM* **36** 373
[19] Tokiai T and Uesugi T 1995 *J. Am. Ceram. Soc.* **78** 1089
[20] Tokiai T, Uesugi T, Nosaka M, Hirayama A, Ito K and Koumoto K 1997 *J. Mater. Sci.* **32** 3007